

Isogeometric Residual Minimization Method (iGRM) with Direction Splitting Preconditioner for Stationary Advection-Diffusion Problems

M. Łoś⁽¹⁾, Q.Deng⁽³⁾, I. Muga⁽²⁾, V.M.Calo^(3,4), M. Paszyński⁽¹⁾

*(1) Department of Computer Science,
AGH University of Science and Technology, Krakow, Poland
e-mail: paszynsk@agh.edu.pl
e-mail: marcin.los.91@gmail.com*

*(2) Institute of Mathematics,
Pontifical Catholic Univeristy of Valparaíso, Chile
e-mail: ignacio.muga@pucv.cl*

*(3) Applied Geology, Faculty of Science and Engineering, Curtin University, Perth, WA, Australia,
e-mail: victor.calo@curtin.edu.au*

*(4) Mineral Resources, Commonwealth Scientific and Industrial Research Organisation (CSIRO),
Kensington, WA, Australia 6152*

Abstract

In this paper, we propose the Isogeometric Residual Minimization (iGRM) with direction splitting. The method mixes the benefits resulting from isogeometric analysis, residual minimization, and alternating direction solver. Namely, we utilize tensor product B-spline basis functions and alternating direction methods. We apply a stabilized mixed method based on residual minimization. We propose a preconditioned conjugate gradients method with a linear computational cost resulting from a Kronecker product structure of the system of linear equations. We test our method on two-dimensional simulations of advection-diffusion problems, including the problem with the manufactured solution, the Eriksson-Johnson problem, and a rotating flow problem. We compare our method to the Discontinuous Petrov-Galerkin and the Streamline Upwind Petrov-Galerkin (SUPG) stabilization methods. The resulting method is not restricted to a Kronecker product structure of the diffusion or advection data.

Keywords: isogeometric analysis, residual minimization, iteration solvers, advection-diffusion simulations, linear computational cost, preconditioners

1. Introduction

The alternating directions method (ADS) is discussed, among many other sources, in [1–6] and solves finite differences parabolic and hyperbolic problems. A modern version of this method solves different classes of problems [7, 8].

Isogeometric analysis (IGA) [9] bridges the gap between the Computer Aided Design (CAD) and Computer Aided Engineering (CAE) communities. The idea of IGA is to apply spline [10] basis functions to the construction to the finite element method (FEM). IGA has multiple applications in time-dependent simulations, including phase-field models [11, 12], phase-separation simulations with application to cancer growth simulations [13, 14], wind turbine aerodynamics [15], incompressible hyper-elasticity [16], turbulent flow simulations [17], transport of drugs in cardiovascular applications [18] or the blood flow simulations and drug transport in arteries simulations [19–21].

Recently, the direction splitting method was applied [22–24] for fast solution of the projection problem with isogeometric analysis. The direction splitting method delivers fast simulations for explicit dynamics [25–29]. For tensor product grids the explicit time integration scheme with isogeometric discretization is equivalent to the solution of a sequence of isogeometric L2 projections.

The minimum residual methods aim to find $u_h \in U_h$ such that

$$u_h = \operatorname{argmin}_{w_h \in U_h} \|b(w_h, \cdot) - \ell(\cdot)\|_{V^*} ,$$

where U and V are Hilbert spaces, $b : U \times V \rightarrow \mathbb{R}$ is a continuous bilinear (weak) form, $U_h \subset U$ is a discrete trial space, and $\ell \in V'$ is a given right-hand side. Several discretization techniques are particular incarnations of this wide-class of residual minimization methods. These include: the *least-squares finite element method* [30], the *discontinuous Petrov-Galerkin method (DPG) with optimal test functions* [31], the *variational stabilization method* [32], or the *automatic variationally stable finite element method* [33]. We propose residual minimization techniques which exploit the tensor product structure of the discrete space to deliver fast and reliable Uzawa-like iteration schemes to solve the resulting global system in few iterations. We approach the residual minimization as a saddle point (mixed) formulation, as described in [35]. We exploit the Kronecker product structure of the isogeometric residual minimization method to obtain a linear computational cost preconditioner for conjugate gradients solver (CG).

In this paper, we describe the benefits we obtain from designing a method that blends isogeometric analysis, residual minimization, and the alternating directions

solver. We call our method isogeometric Residual Minimization (iGRM) with direction splitting preconditioner.

We apply our method to the solution of stationary advection-diffusion problems. We test our method on four stationary computational problems, including the problem with the manufactured solution, the Eriksson-Johnson model problem, and the circular wind problem.

2. The Isogeometric Residual Minimization Method (iGRM)

For the sake of simplicity, we focus on a two-dimensional model in space, but the formulation can be easily extended to three-dimensions.

2.1. Residual minimization method for the global problem

For a general weak problem: Find $u \in U$ such as

$$b(u, v) = l(v) \quad \forall v \in V \quad (1)$$

we define the operator $B : U \rightarrow V'$ such as $\langle Bu, v \rangle_{V' \times V} = b(u, v)$.

$$B : U \rightarrow V' \quad (2)$$

such that

$$\langle Bu, v \rangle_{V' \times V} = b(u, v) \quad (3)$$

so we can reformulate the problem as

$$Bu - l = 0 \quad (4)$$

We wish to minimize the residual

$$u_h = \operatorname{argmin}_{w_h \in U_h} \frac{1}{2} \|Bw_h - l\|_{V'}^2 \quad (5)$$

We introduce the Riesz operator as

$$R_V : V \ni v \rightarrow (v, \cdot) \in V' \quad (6)$$

We can project the problem back to V

$$u_h = \operatorname{argmin}_{w_h \in U_h} \frac{1}{2} \|R_V^{-1}(Bw_h - l)\|_V^2 \quad (7)$$

The minimum is attained at u_h when the Gâteaux derivative is equal to 0 in all directions:

$$\langle R_V^{-1}(Bu_h - l), R_V^{-1}(Bw_h) \rangle_V = 0 \quad \forall w_h \in U_h \quad (8)$$

We define the residual $r = R_V^{-1}(Bu_h - l)$ and our problem is reduced to

$$\langle r, R_V^{-1}(Bw_h) \rangle = 0 \quad \forall w_h \in U_h \quad (9)$$

which is equivalent to

$$\langle Bw_h, r \rangle = 0 \quad \forall w_h \in U_h. \quad (10)$$

From the definition of the error representation in term of the residual we have

$$(r, v)_V = \langle Bu_h - l, v \rangle \quad \forall v \in V. \quad (11)$$

Thus, our problem reduces to the following semi-infinite problem: Find $(r, u_h)_{V \times U_h}$ such as

$$\begin{aligned} (r, v)_V - \langle Bu_h - l, v \rangle &= 0 \quad \forall v \in V \\ \langle Bw_h, r \rangle &= 0 \quad \forall w_h \in U_h \end{aligned} \quad (12)$$

We discretize the test space $V_m \in V$ to get the discrete problem: Find $(r_m, u_h)_{V_m \times U_h}$ such as

$$\begin{aligned} (r_m, v_m)_{V_m} - \langle Bu_h - l, v_m \rangle &= 0 \quad \forall v \in V_m \\ \langle Bw_h, r_m \rangle &= 0 \quad \forall w_h \in U_h \end{aligned} \quad (13)$$

where $(*, *)_{V_m}$ is an inner product in V_m , $\langle Bu_h, v_m \rangle = b(u_h, v_m)$, $\langle Bw_h, r_m \rangle = b(w_h, r_m)$.

Remark 1. We define the discrete test space V_m to be sufficiently close to the abstract V space, to ensure stability, in a sense that the discrete inf-sup condition is satisfied. Thus, we can gain stability enriching the test space V_m while fixing the trial space U_h .

2.2. Minimal residual discretization for the global problem with B-splines

We approximate the solution as tensor products of one dimensional B-splines basis functions of uniform order p in all directions to simplify the discussion. We denote the basis functions in the x -direction for the discrete trial and tests spaces as n_a and N_A , respectively. Similarly, we denote the basis functions in the y -direction for the discrete trial and tests spaces as m_b and M_B , respectively. To simplify the notation, we assume that basis functions for the trial space have the same polynomial

order p in both directions with continuity $p - 1$, in our tests. Additionally, the basis of the trial space has polynomial order $q \geq p$ with continuity $k \leq p - 1$. Thus, we write the discrete trial functions as:

$$\begin{aligned} w_h &= \sum_{a,b} u_{ab} n_a m_b \\ u_h &= \sum_{a,b} w_{ab} n_a m_b \end{aligned} \tag{14}$$

and the tests functions as

$$\begin{aligned} v_h &= \sum_{A,B} v_{AB} N_A M_B \\ r_h &= \sum_{A,B} r_{AB} N_A M_B \end{aligned} \tag{15}$$

3. Conjugate Gradients method for the isogeometric residual minimization

In this Section we derive an iterative algorithm to solve the resulting residual minimization problem. We denote by Ω the bounded open set of \mathbb{R}^d with Lipschitz continuous boundary $\partial\Omega$, where $d = 2, 3$. The advection-diffusion-reaction equation reads

$$\begin{aligned} -\nabla \cdot (\kappa \nabla u) + \mathbf{b} \cdot \nabla u + cu &= f \quad \text{in } \Omega \\ u &= 0 \quad \text{on } \partial\Omega, \end{aligned} \tag{16}$$

where we assume sufficient regularity of the solution.

The corresponding linear matrix system of the residual minimization method is

$$\begin{bmatrix} A & B \\ B^T & 0 \end{bmatrix} \begin{bmatrix} r \\ u \end{bmatrix} = \begin{bmatrix} F \\ 0 \end{bmatrix}, \tag{17}$$

where the terms are arising from isogeometric discretization of (16) with respect to the minimization of the energy norm A , which is defined as

$$A = M + \eta K \tag{18}$$

with

$$\begin{aligned} M &= M_x \otimes M_y, \\ K &= K_x \otimes M_y + M_x \otimes K_y. \end{aligned} \tag{19}$$

From (18), we have

$$\begin{aligned} A &= M + \eta K \\ &= (M_x + \eta K_x) \otimes (M_y + \eta K_y) - \eta^2 K_x \otimes K_y. \end{aligned} \quad (20)$$

Now we approximate A by

$$\tilde{A} = (M_x + \eta K_x) \otimes (M_y + \eta K_y) := A + \tilde{K}. \quad (21)$$

and substitute this into (17).

3.1. Iterative algorithm

We derive an iterative method for solving (17). Firstly, from (17) for a given approximate solution u^k and a residual t^k , we consider iteration residuals to be

$$\begin{aligned} t^k &= F - Ar^k - Bu^k \\ s^k &= -B^T r^k. \end{aligned} \quad (22)$$

Since we partitioned $A = \tilde{A} - \tilde{K}$, we get

$$\begin{aligned} t^k &= F + \tilde{K}r^k - \tilde{A}r^k - Bu^k, \\ s^k &= -B^T r^k. \end{aligned} \quad (23)$$

To solve this system we introduce a predictor-multi-corrector scheme. We build a dual problem, which resembles the features of a preconditioner. We define

$$\begin{aligned} d^k &:= r - r^k \\ c^k &:= u - u^k \end{aligned} \quad (24)$$

Ideally, these could be computed from

$$\begin{bmatrix} A & B \\ B^T & 0 \end{bmatrix} \begin{bmatrix} d^k \\ c^k \end{bmatrix} = \begin{bmatrix} t^k \\ s^k \end{bmatrix}, \quad (25)$$

namely

$$\begin{aligned} Ad^k + Bc^k &= A(r - r^k) + B(u - u^k) \\ &= Ar + Bu - Ar^k - Bu^k \\ &= F - Ar^k - Bu^k = t^k \\ B^T d^k &= B^T(r - r^k) \\ &= B^T r - B^T r^k = -B^T r^k = s^k \end{aligned} \quad (26)$$

We however do not know how to solve the (25) fast, so in our iterative procedure we replace A by \tilde{A} .

$$\begin{bmatrix} \tilde{A} & B \\ B^T & 0 \end{bmatrix} \begin{bmatrix} d^k \\ c^k \end{bmatrix} = \begin{bmatrix} t^k \\ s^k \end{bmatrix}, \quad (27)$$

We solve now the dual problem

$$\begin{bmatrix} \tilde{A}^{-1}\tilde{A} & \tilde{A}^{-1}B \\ B^T & 0 \end{bmatrix} \begin{bmatrix} d^k \\ c^k \end{bmatrix} = \begin{bmatrix} \tilde{A}^{-1}t^k \\ s^k \end{bmatrix}, \quad (28)$$

We subtract the first equation multiplied by B^T from the second

$$\begin{bmatrix} I & \tilde{A}^{-1}B \\ 0 & -B^T\tilde{A}^{-1}B \end{bmatrix} \begin{bmatrix} d^k \\ c^k \end{bmatrix} = \begin{bmatrix} \tilde{A}^{-1}t^k \\ s^k - B^T\tilde{A}^{-1}t^k \end{bmatrix}, \quad (29)$$

We substitute the residual from (23) to the first equation in (29) to get

$$\begin{aligned} d^k + \tilde{A}^{-1}Bc^k &= \tilde{A}^{-1}(F - \tilde{A}r^k + \tilde{K}r^k - Bu^k) \\ &= \tilde{A}^{-1}F - \tilde{A}^{-1}\tilde{A}r^k + \tilde{A}^{-1}\tilde{K}r^k - \tilde{A}^{-1}Bu^k \end{aligned} \quad (30)$$

We introduce

$$\begin{aligned} \delta d^k &= \tilde{A}^{-1}(F + \tilde{K}r^k - Bu^k), \\ \delta c^k &= -B^T\delta d^k. \end{aligned} \quad (31)$$

to get

$$d^k + \tilde{A}^{-1}Bc^k = \tilde{A}^{-1}(-\tilde{A}r^k) + \delta d^k = -r^k + \delta d^k \quad (32)$$

so

$$d^k = -r^k + \delta d^k - \tilde{A}^{-1}Bc^k \quad (33)$$

Now, we substitute the residual from (23), the definition of δd^k from (31) into the second equation in (29), and by using (22), we get

$$\begin{aligned} -B^T\tilde{A}^{-1}Bc^k &= s^k - B^T\tilde{A}^{-1}t^k \\ &= s^k - B^T\tilde{A}^{-1}(F - \tilde{A}r^k + \tilde{K}r^k - Bu^k) \\ &= s^k - B^T\delta d^k + B^T r^k \\ &= -B^T\delta d^k = -\delta c^k \end{aligned} \quad (34)$$

Thus, the resulting update becomes

$$\begin{aligned} d^k &= -r^k + \delta d^k - \tilde{A}^{-1}Bc^k \\ B^T\tilde{A}^{-1}Bc^k &= B^T\delta d^k = \delta c^k \end{aligned} \quad (35)$$

Here the first equation is a primal update and the second equation is solved using a Conjugate-Gradient (CG) type method. Since \tilde{A} has a Kronecker product structure (20), and we use B-spline basis functions for the discretizations, the factorizations of the \tilde{A} matrix has a linear computational cost. This is because the Kronecker product matrices can be factorized in two steps. In the first step we factorize the first Kronecker product sub-matrix $(M_x + \eta K_x)$, while in the second sub-step we factorize the second sub-matrix $(M_y + \eta K_y)$, both of linear cost with respect to their one dimensional set of unknowns. Thus, these matrices are $2p + 1$ diagonal, where p stands for the B-spline order, and the total cost of factorization is linear (c.f., [24, 25] for more details). Thus, the cost of the application of the preconditioner is linear.

Algorithm 1 describes the overall iterative solution scheme (17). The u^k and r^k stands for the iterative solutions of our residual minimization problem. The inner loop represents the CG algorithm, used to compute u^{k+1} , where p^j and q^j are the search directions. In the CG algorithm, the search direction is initialized with δc^k , and the update to the residual r^{k+1} uses δd^k .

Algorithm 1 Inner-Outer Iterative Method

Initialize $\{u^0 = 0; r^0 = 0\}$

for $k = 1 \rightarrow N$ until convergence **do**

Initialize $\{q^{(0)} = p^{(0)} = \delta c^k; u^{(0)} = u^k\}$

for $j = 1 \rightarrow N_k$ until convergence **do**

Calculate in a sequence

$$\begin{aligned}\theta^{(j)} &= Bp^{(j)}; \\ \delta^{(j)} &= \tilde{A}^{-1}\theta^{(j)}; \\ \alpha^{(j)} &= \frac{(p^{(j)}, q^{(j)})}{(\theta^{(j)}, \delta^{(j)})}; \\ u^{(j+1)} &= u^{(j)} + \alpha^{(j)}p^{(j)}; \\ q^{(j+1)} &= q^{(j)} - \alpha^{(j)}B^T\delta^{(j)}; \\ \beta^{(j+1)} &= \frac{(q^{(j+1)}, q^{(j+1)})}{(q^{(j)}, q^{(j)})}; \\ p^{(j+1)} &= q^{(j+1)} + \beta^{(j+1)}p^{(j)}; \\ j &= j + 1;\end{aligned}\tag{36}$$

end for

Calculate in a sequence

$$\begin{aligned}c^k &= u^{(N_k)} - u^{(0)}; \\ u^{k+1} &= u^{(N_k)}; \\ r^{k+1} &= \tilde{A}^{-1}Bc^k + \delta d^k; \\ k &= k + 1; \\ \delta d^{k+1} &= \tilde{A}^{-1}(F + \tilde{K}r^{k+1} - Bu^{k+1}); \\ \delta c^{k+1} &= -B^T\delta d^{k+1}.\end{aligned}\tag{37}$$

end for

To determine the convergence, for the inner loop, we iterative until $\alpha^{(j+1)} \leq \textit{tolerance}$, and denote this iteration as j_c . The outer iteration calculates

$$\begin{aligned} c^k &= u^{(j_c)} - u^{(0)}; \\ u^{k+1} &= u^{(j_c)}; \\ w^{k+1} &= \delta d^k + \tilde{A}^{-1} B c^k. \end{aligned} \tag{38}$$

The outer iteration stops at $c^{k+1} \leq \textit{tolerance}$.

3.2. Convergence of the iterative algorithm

Since the inner loop of **Algorithm 1** is essentially a preconditioned CG and both the CG and preconditioned CG have been proven to be convergent (see, for example, [41]), we focus on the spectral analysis of (37) in **Algorithm 1**.

Applying the initialization $u^{(0)} = u^k$ of the inner loop in **Algorithm 1** and using the first two equations of (37), we obtain

$$u^{k+1} = u^k + c^k \tag{39}$$

where c^k is the update of u^k .

Similarly, using the third and fourth equations of (37), we obtain

$$r^{k+1} = \tilde{A}^{-1}(F + \tilde{K}r^k - Bu^k) - \tilde{A}^{-1}Bc^k. \tag{40}$$

To simplify the spectral analysis and without loss of generality we set $F = 0$. Thus, combining (39) and (40) gives

$$\begin{bmatrix} u^{k+1} \\ r^{k+1} \end{bmatrix} = \begin{bmatrix} 1 & 0 \\ -\tilde{A}^{-1}B & \tilde{A}^{-1}\tilde{K} \end{bmatrix} \begin{bmatrix} u^k \\ r^k \end{bmatrix} + \begin{bmatrix} c^k \\ -\tilde{A}^{-1}Bc^k \end{bmatrix}. \tag{41}$$

Let $\eta = h^2$. Now, we analyze the spectrum of

$$\tilde{A}^{-1}\tilde{K} = (M_x + h^2K_x)^{-1} \otimes (M_y + h^2K_y)^{-1} \cdot (h^2K_x \otimes h^2K_y). \tag{42}$$

We apply the spectral decomposition [42] of matrix K_ξ , $\xi = x, y$ with respect to M_ξ and arrive at

$$K_\xi = M_\xi P_\xi D_\xi P_\xi^{-1}, \tag{43}$$

where D_ξ is a diagonal matrix with entries to be the eigenvalues of the generalized eigenvalue problem

$$K_\xi v_\xi = \lambda_\xi M_\xi v_\xi \tag{44}$$

and P_ξ is a matrix with all the columns being the eigenvectors. We assume that all the eigenvalues are sorted in ascending order and are listed in D_ξ and the j -th column of P_ξ is associated with the eigenvalue $\lambda_{\xi,j} = D_{\xi,jj}$.

Using (43) and (21), we now calculate

$$\begin{aligned}\tilde{A}^{-1} &= (M_x + h^2 K_x)^{-1} \otimes (M_y + h^2 K_y)^{-1} \\ &= (M_x + h^2 M_x P_x D_x P_x^{-1})^{-1} \otimes (M_y + h^2 M_y P_y D_y P_y^{-1})^{-1} \\ &= P_x E_x P_x^{-1} M_x^{-1} \otimes P_y E_y P_y^{-1} M_y^{-1},\end{aligned}\tag{45}$$

where

$$E_\xi = (I + h^2 D_\xi)^{-1}, \quad \xi = x, y.\tag{46}$$

We assume here that the mesh is uniform in both directions.

Thus, similarly we have

$$\begin{aligned}\tilde{A}^{-1} \tilde{K} &= (P_x E_x P_x^{-1} M_x^{-1} \otimes P_y E_y P_y^{-1} M_y^{-1}) \\ &\quad \cdot (h^2 M_x P_x D_x P_x^{-1} \otimes h^2 M_y P_y D_y P_y^{-1}) \\ &= (P_x \otimes P_y) \cdot (h^2 E_x D_x \otimes h^2 E_y D_y) \cdot (P_x^{-1} \otimes P_y^{-1}) \\ &= (P_x \otimes P_y) \cdot (h^2 (I + h^2 D_x)^{-1} D_x \otimes h^2 (I + h^2 D_y)^{-1} D_y) \cdot (P_x^{-1} \otimes P_y^{-1}).\end{aligned}\tag{47}$$

The middle term is a diagonal matrix. Thus, a typical eigenvalue of $\tilde{A}^{-1} \tilde{K}$ is

$$\lambda = \frac{h^4 \lambda_{x,i} \lambda_{y,j}}{(1 + h^2 \lambda_{x,i})(1 + h^2 \lambda_{y,i})},\tag{48}$$

where i, j are indices of eigenvalues in each dimension. The spectral radius of $\tilde{A}^{-1} \tilde{K}$ is then

$$\rho = \frac{h^4 \lambda_{x,\max} \lambda_{y,\max}}{(1 + h^2 \lambda_{x,\max})(1 + h^2 \lambda_{y,\max})},\tag{49}$$

where $\lambda_{\xi,\max}$, $\xi = x, y$ are the maximum eigenvalues in each dimension. Immediately, we have

$$0 < \lambda \leq \rho < 1.\tag{50}$$

Thus, the eigenvalues of the amplifying block-matrix (the vector in terms of c^k is from inner CG) in (41) are 1 and λ , which are bounded by 1 and the eigenvalues of their powers are also bounded by 1. Hence, the iterative **Algorithm 1** is convergent.

4. Numerical results for stationary problems

4.1. A manufactured solution problem

We focus on a model problem with a manufactured solution. For a unitary square domain $\Omega = (0, 1)^2$, the advection vector $\beta = (1, 1)^T$, and $Pe = 100, \epsilon = 1/Pe$ we seek the solution of the advection-diffusion equation

$$\frac{\partial u}{\partial x} + \frac{\partial u}{\partial y} - \epsilon \left(\frac{\partial^2 u}{\partial x^2} + \frac{\partial^2 u}{\partial y^2} \right) = f \quad (51)$$

with Dirichlet boundary conditions $u = g$ on the whole of $\Gamma = \partial\Omega$. We utilize a manufactured solution

$$u(x, y) = \left(x + \frac{e^{Pe*x} - 1}{1 - e^{Pe}} \right) \left(y + \frac{e^{Pe*y} - 1}{1 - e^{Pe}} \right)$$

enforced by the right-hand side, and we use homogeneous Dirichlet boundary conditions on $\partial\Omega$.

We introduce first the weak formulation

$$b(u, v) = l(v) \quad \forall v \in V \quad (52)$$

$$\begin{aligned} b(u, v) = & \left(\frac{\partial u}{\partial x}, v \right)_{\Omega} + \left(\frac{\partial u}{\partial y}, v \right)_{\Omega} + \epsilon \left(\frac{\partial u}{\partial x}, \frac{\partial v}{\partial x} \right)_{\Omega} + \epsilon \left(\frac{\partial u}{\partial y}, \frac{\partial v}{\partial y} \right)_{\Omega} \\ & - \left(\epsilon \frac{\partial u}{\partial x} n_x, v \right)_{\Gamma} - \left(\epsilon \frac{\partial u}{\partial y} n_y, v \right)_{\Gamma} \\ & - (u, \epsilon \nabla v \cdot n)_{\Gamma} - (u, \beta \cdot nv)_{\Gamma} - (u, 3p^2 \epsilon / hv)_{\Gamma} \end{aligned}$$

where $n = (n_x, n_y)$ is the versor normal to Γ , and h is the element diameter,

$$l(v) = (f, v)_{\Omega} - (g, \epsilon \nabla v \cdot n)_{\Gamma} - (g, \beta \cdot nv)_{\Gamma} - (g, 3p^2 \epsilon / hv)_{\Gamma} \quad (53)$$

where the **red** terms correspond to the weak imposition of the Dirichlet boundary conditions on Γ and we set $g = 0$ here, and f corresponds to the manufactured solution, and the **blue** terms resulting from the integration by parts, which are often denoted as consistency terms [46], and the gray represents the penalty terms.

In our problem we seek the solution in space $U = V = H^1(\Omega)$. The inner product in V is defined as

$$(u, v)_V = (u, v)_{L_2} + \left(\frac{\partial u}{\partial x}, \frac{\partial v}{\partial x} \right)_{L_2} + \left(\frac{\partial u}{\partial y}, \frac{\partial v}{\partial y} \right)_{L_2} \quad (54)$$

We plug the weak form (52) and the inner product (54) into the iGRM setup (13) and we use the preconditioned CG solver described in Section 3.

In this problem we study the h - and p -convergence of the iGRM method on uniform grids, using different combinations of trial and test functions. We do not employ adaptive Shishkin grids here [34]. We increase the accuracy by increasing the order and continuity of trial spaces (k -refinement [9, 48]), and by testing with quadratic C^0 B-splines, since increasing the test space further does not improve the accuracy of the solution. Nevertheless, increasing trial space order and continuity improves the accuracy of the solution. Similarly, refining the mesh also improves the accuracy of the solution.

Table 1 illustrates the h and p -convergence of the method. The rows represent p -refinement of the trial test, from $(p, p-1)$ to $(p+1, p)$, and the columns represent h -refinement, from $n \times n$ mesh to $2n \times 2n$ mesh. The p refinement with fixed test space $(2, 0)$ increases the problem size from $(n+p) \times (n+p) + (n+2) \times (n+2)$ to $(n+p+1) \times (n+p+1) + (n+2) \times (n+2)$, while the h refinement with fixed test space $(2, 0)$ increases the problem size from $(n+p) \times (n+p) + (n+2) \times (n+2)$ to $(2n+p) \times (2n+p) + (2n+2) \times (2n+2)$, which makes the higher continuity grids attractive.

4.2. Problem 2 with boundary layer

In the second problem we solve advection-diffusion equations

$$\frac{\partial u}{\partial x} + \frac{\partial u}{\partial y} - \epsilon \left(\frac{\partial^2 u}{\partial x^2} + \frac{\partial^2 u}{\partial y^2} \right) = 1 \quad (55)$$

over the square domain $\Omega = (0, 1)^2$, the right-hand side $f = 1$, the advection vector $\beta = (1, 1)^T$, with zero Dirichlet boundary conditions. We use the Peclet number $Pe = 1/\epsilon = 10^6$. Again, we use weak imposition of Dirichlet boundary conditions.

The weak formulation

$$b(u, v) = l(v) \quad \forall v \in V \quad (56)$$

$$\begin{aligned} b(u, v) = & \left(\frac{\partial u}{\partial x}, v \right)_{\Omega} + \left(\frac{\partial u}{\partial y}, v \right)_{\Omega} + \epsilon \left(\frac{\partial u}{\partial x}, \frac{\partial v}{\partial x} \right)_{\Omega} + \epsilon \left(\frac{\partial u}{\partial y}, \frac{\partial v}{\partial y} \right)_{\Omega} \\ & - \left(\epsilon \frac{\partial u}{\partial x} n_x, v \right)_{\Gamma} - \left(\epsilon \frac{\partial u}{\partial y} n_y, v \right)_{\Gamma} \\ & - (u, \epsilon \nabla v \cdot n)_{\Gamma} - (u, \beta \cdot nv)_{\Gamma} - (u, 3p^2 \epsilon / hv)_{\Gamma} \end{aligned}$$

n	trial(2,1) test(2,0)	trial(3,2) test(2,0)	trial(4,3) test(2,0)	trial(5,4) test(2,0)
#DOF	389	410	433	458
L2	192	151	78	28
H1	101	74	44	32
8×8				
#DOF	1413	1450	1489	1530
L2	80	16	3.29	1.48
H1	59	29	18	10
16×16				
#DOF	5381	5450	5521	5594
L2	32	1.33	0.27	0.056
H1	31	9.77	3.16	0.82
32×32				
#DOF	20997	21130	21265	21402
L2	7.66	0.07	0.01	0.003
H1	9.86	1.67	0.26	0.068
64×64				

0.0 0.2 0.4 0.6 0.8 1.0

Table 1: Solution of Problem 1 by iGRM method,¹⁴ with different trial and test spaces, for different mesh dimensions.

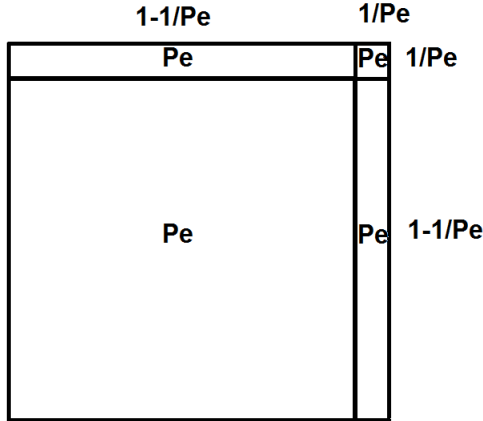


Figure 1: 2×2 mesh related to the Pecklet number Pe .

where $n = (n_x, n_y)$ is the versor normal to Γ , the second line corresponds to the consistency terms and the third line corresponds to the symmetric interior penalty terms of Nitsche [46].

$$l(v) = (1, v)_\Omega \quad (57)$$

We use 2×2 Shishkin mesh [34] presented in Figure 1. In this problem we study the quality of the solution for large Pecklet numbers, e.g. $Pe = 10^6$ on simple 2×2 mesh, using different combinations of trial and test functions. The numerical results are summarized in Figure 2.

4.3. Eriksson-Johnson model problem

Let us focus on the model Eriksson-Johnson problem with the modifications proposed by [35]. For the square domain $\Omega = (0, 1)^2$ and the advection vector $\beta = (1, 0)^T$, we seek the solution of the advection-diffusion equation

$$\frac{\partial u}{\partial x} - \epsilon \left(\frac{\partial^2 u}{\partial x^2} + \frac{\partial^2 u}{\partial y^2} \right) = 0 \quad (58)$$

We partition the boundary $\Gamma = \partial\Omega$ into the inflow $\Gamma^- = \{x \in \Gamma : b \cdot n < 0\} = \{(x, y) : x * y = 0\}$ and the outflow $\Gamma^+ = \{x \in \Gamma : b \cdot n \geq 0\}$. We introduce Dirichlet boundary conditions

$$\begin{aligned} u &= g = \sin(\Pi y) \text{ for } x \in \Gamma^- \\ u &= 0 \text{ for } x \in \Gamma^+ \end{aligned}$$

weakly on the boundary Γ . The problem is driven by the inflow Dirichlet boundary condition and develops a boundary layer of width ϵ at the outflow $x = 1$.

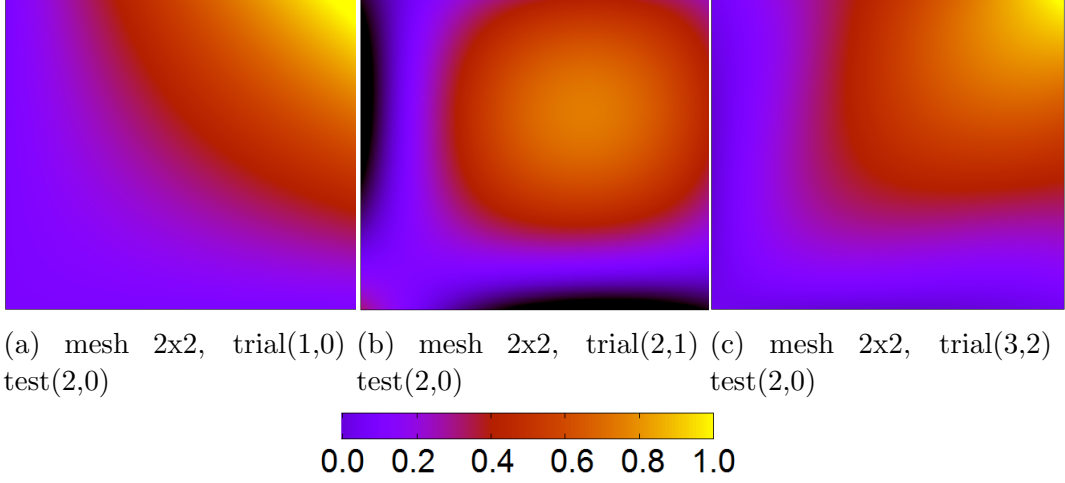


Figure 2: Solutions of the Problem 2 over the mesh with 2×2 elements presented in Figure 1 for different trial $(p,p-1)$ and for test $(2,0)$ B-spline basis functions.

We introduce first the weak formulation for the Eriksson-Johnson problem

$$b(u, v) = l(v) \quad \forall v \in V \quad (59)$$

$$\begin{aligned} b(u, v) = & \left(\frac{\partial u}{\partial x}, v \right) + \epsilon \left(\frac{\partial u}{\partial x}, \frac{\partial v}{\partial x} \right) + \epsilon \left(\frac{\partial u}{\partial y}, \frac{\partial v}{\partial y} \right) \\ & - \left(\epsilon \frac{\partial u}{\partial x} n_x, v \right)_{\Gamma} - \left(\epsilon \frac{\partial u}{\partial y} n_y, v \right)_{\Gamma} \\ & - (u, \epsilon \nabla v \cdot n)_{\Gamma} - (u, \beta \cdot nv)_{\Gamma} - (u, 3p^2 \epsilon / hv)_{\Gamma} \end{aligned}$$

$$l(v) = - (g, \epsilon \nabla v \cdot n)_{\Gamma^-} - (g, \beta \cdot nv)_{\Gamma^-} - (g, 3p^2 \epsilon / hv)_{\Gamma^-} \quad (60)$$

In this problem, we test the residual minimization method applied for the Eriksson-Johnson problem on a 2×2 simple Shishkin mesh presented in Figure 3. We refine the mesh by breaking these four elements in the Shishkin mesh manner as described in [34].

We compare with residual minimization method [35] using Lagrange $(2,0)$ polynomials for trial and $(3,0)$ polynomials for testing. In our method, we use $(2,1)$ trial B-splines with $(3,0)$ test B-splines. Thus, our trial spaces have higher continuity and are smaller, and the test spaces are selected to be identical to those used in [35]. The numerical results are presented in Figures 2-3, for $Pe = 10^4$ and $Pe = 10^6$. The

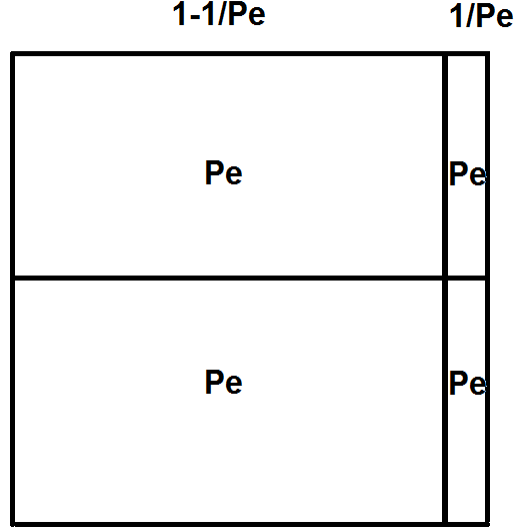


Figure 3: 2×2 mesh for the Eriksson problem.

convergence in L_2 and H_1 norms is summarized in Tables 4 and 5. When comparing with [35], we use the information in Figure 5.3, where L_2 is plotted for $Pe = 10^4$ and $Pe = 10^6$. We first compare our method against the one presented in [35] for $Pe = 10^4$. For comparable mesh sizes, in the order of 2000 DOFs, the errors are comparable. But for $Pe = 10^6$ iGRM delivers an error which is about an order of magnitude smaller. Thus, we conclude that for higher order B-splines the residual minimization delivers better accuracy for higher Pecklet numbers.

A commonly used stabilization technique is the SUPG method [36, 37] In this method we modify the weak form in the following way

$$b(u, v) + (R(u), \tau \beta \cdot \nabla v) = l(v) \quad \forall v \in V \quad (61)$$

where $R(u) = \frac{\partial u}{\partial x} + \epsilon \Delta u$, and $\tau^{-1} = \left(\frac{\beta_x}{h_x} + \frac{\beta_y}{h_y} \right) + 3\epsilon \frac{1}{h_x^2 + h_y^2}$, where in our case diffusion term $\epsilon = 10^{-6}$, and convection term $\beta = (1, 0)$, and h_x and h_y are horizontal and vertical dimensions of an element. Thus, we have

$$b_{SUPG}(u, v) = l(v) \quad \forall v \in V \quad (62)$$

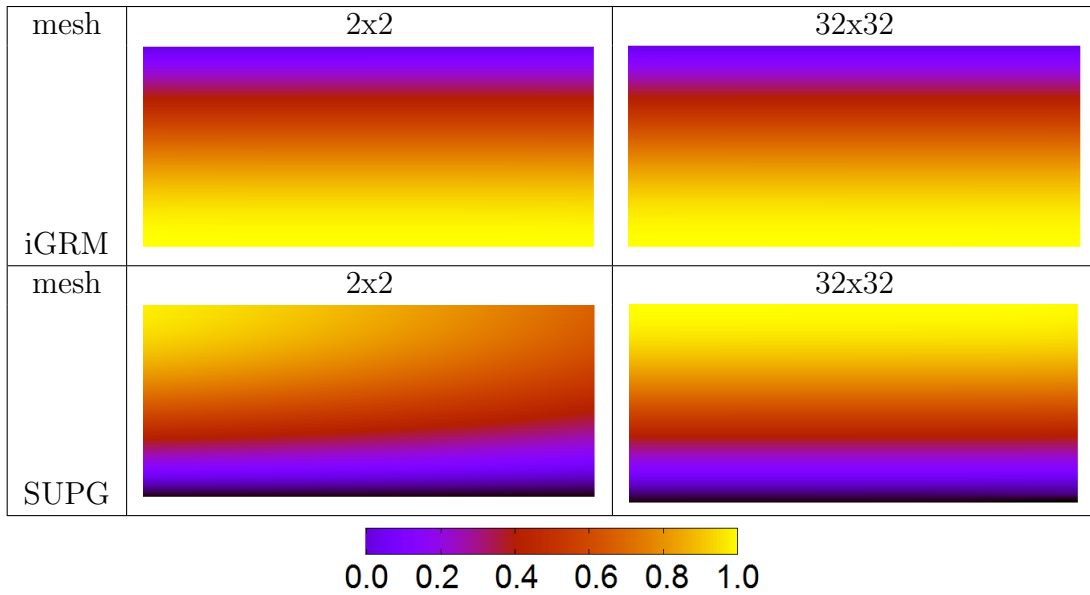


Table 2: iGRM (top) and SUPG (bottom) solutions of the Eriksson-Johnsson by using iGRM methods for $Pe=10000$ with (2,1) for trial and (3,0) for testing, on 2x2, and 32x32 grids.

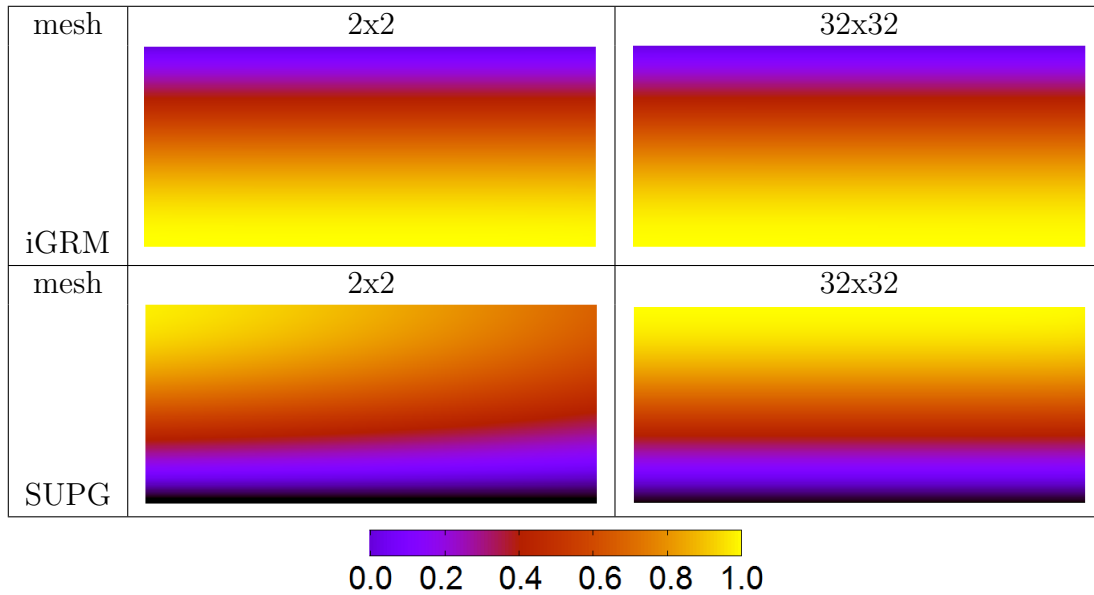


Table 3: iGRM (top) and SUPG (bottom) solutions of the Eriksson-Johnsson by using iGRM methods for $Pe=1,000,000$ with (2,1) for trial and (3,0) for testing, on 2x2, and 32x32 grids.

n	iGRM (2,1) (2,0)			iGRM (2,1) (3,0)			SUPG		
	#NDOF	L2	H1	#NDOF	L2	H1	#NDOF	L2	H1
2	41	98.500	74.356	65	2.537	26.449	16	13.508	25.119
4	117	0.26	21.11	205	0.308	20.807	36	6.724	19.33
8	389	0.0664	7.444	725	0.0681	7.268	100	1.884	6.148
16	1413	0.0291	2.632	2725	0.0227	2.613	324	0.4835	2.107
32	5381	0.00996	0.906	10565	0.00955	0.906	1156	0.2778	1.177

Table 4: Comparison of the iGRM and SUPG methods starting on 2×2 grid presented in Figure 3, for the Eriksson-Johnson problem with $Pe = 10000$.

n	iGRM (2,1) (2,0)			iGRM (2,1) (3,0)			SUPG		
	#NDOF	L2	H1	#NDOF	L2	H1	#NDOF	L2	H1
2	41	99.029	74.5	65	2.444	26.407	16	13.519	25.134
4	117	0.207	21.249	205	0.259	20.905	36	6.725	19.366
8	389	0.0268	7.490	725	0.033	7.305	100	1.885	6.164
16	1413	0.00383	2.657	2725	0.00453	2.634	324	0.483	2.114
32	5381	0.000734	0.922	10565	0.000793	0.920	1156	0.1229	0.693

Table 5: Comparison of the iGRM and SUPG methods starting on 2×2 grid presented in Figure 3, for the Eriksson-Johnson problem with $Pe = 1,000,000$.

$$\begin{aligned}
b^{SUPG}(u, v) = & \left(\frac{\partial u}{\partial x}, v \right) + \epsilon \left(\frac{\partial u}{\partial x}, \frac{\partial v}{\partial x} \right) + \epsilon \left(\frac{\partial u}{\partial y}, \frac{\partial v}{\partial y} \right) \\
& - \left(\epsilon \frac{\partial u}{\partial x} n_x, v \right)_{\Gamma} - \left(\epsilon \frac{\partial u}{\partial y} n_y, v \right)_{\Gamma} \\
& - (u, \epsilon \nabla v \cdot n)_{\Gamma} - (u, \beta \cdot nv)_{\Gamma} - (u, 3p^2 \epsilon / hv)_{\Gamma} \\
& + \left(\frac{\partial u}{\partial x} + \epsilon \Delta u, \left(\frac{1}{h_x} + 3\epsilon \frac{1}{h_x^2 + h_y^2} \right)^2 \frac{\partial v}{\partial x} \right)
\end{aligned}$$

As Tables 2 and 3 show, iGRM delivers solutions results that are orders of magnitude better than SUPG. Nevertheless, the resulting algebraic system for iGRM is presently an order of magnitude more expensive than the direct solver solution with MUMPS of the SUPG system. In future work we will report on optimizations that accelerate the resolution of the iterative method we propose.

4.4. Circular wind problem

In the fourth problem we solve a circular flow with the following advection-diffusion equations

$$\beta_x \frac{\partial u}{\partial x} + \beta_y \frac{\partial u}{\partial y} - \epsilon \left(\frac{\partial^2 u}{\partial x^2} + \frac{\partial^2 u}{\partial y^2} \right) = 0 \tag{63}$$

over the rectangular domain $\Omega = (0, 1) \times (-1, 1)$, with zero right-hand side $f = 0$, the advection vector $\beta(x, y) = (\beta_x(x, y), \beta_y(x, y)) = \psi\left(\frac{-y}{(x^2+y^2)^{\frac{1}{2}}}, \frac{x}{(x^2+y^2)^{\frac{1}{2}}}\right)$ modeling the circular wind, where ψ is the wind force coefficient. We introduce $\Gamma_1 = \{(x, y) : x = 0, 0.5 \leq y \leq 1.0\}$, $\Gamma_2 = \{(x, y) : x = 0, 0.0 \leq y \leq 0.5\}$, $\Gamma_3 = \{(x, y) : x = 0, -0.5 \leq y \leq 0.0\}$, $\Gamma_4 = \{(x, y) : x = 0, -1.0 \leq y \leq -0.5\}$, We utilize the Dirichlet boundary conditions $u = g$ on $\Gamma = \partial\Omega$ where

$$g = \frac{1}{2} \left(\tanh \left((|y| - 0.35) \frac{b}{\epsilon} \right) + 1 \right), \text{ for } x \in \Gamma_2 \cup \Gamma_3$$

$$g = \frac{1}{2} \left(0.65 - \tanh \left((|y|) \frac{b}{\epsilon} \right) + 1 \right), \text{ for } x \in \Gamma_1 \cup \Gamma_4 \quad (64)$$

$$g = 0, \text{ for } x \in \Gamma \setminus \Gamma_1 \cup \Gamma_2 \cup \Gamma_3 \cup \Gamma_4 \quad (65)$$

We introduce the Dirichlet boundary condition weakly on the boundary Γ .

The weak formulation

$$b(u, v) = l(v) \quad \forall v \in V \quad (66)$$

$$b(u, v) = \left(\beta_x \frac{\partial u}{\partial x}, v \right)_{\Omega} + \left(\beta_y \frac{\partial u}{\partial y}, v \right)_{\Omega} + \epsilon \left(\frac{\partial u}{\partial x}, \frac{\partial v}{\partial x} \right)_{\Omega} + \epsilon \left(\frac{\partial u}{\partial y}, \frac{\partial v}{\partial y} \right)_{\Omega} \quad (67)$$

$$- \left(\epsilon \frac{\partial u}{\partial x} n_x, v \right)_{\Gamma} - \left(\epsilon \frac{\partial u}{\partial y} n_y, v \right)_{\Gamma} - (u, \epsilon \nabla v \cdot n)_{\Gamma} - (u, \beta \cdot nv)_{\Gamma} - (u, 3p^2 \epsilon / hv)_{\Gamma}$$

where $n = (n_x, n_y)$ is the versor normal to Γ ,

$$l(v) = - (g, \epsilon \nabla v \cdot n)_{\Gamma} - (g, \beta \cdot nv)_{\Gamma} - (g, 3p^2 \epsilon / hv)_{\Gamma} \quad (68)$$

$n = (n_x, n_y)$ is the versor normal to the boundary, and the right-hand side forcing is equal to 0.

We plug the weak form (66) and the inner product (54) into the iGRM setup (13) and we use the preconditioned CG solver described in Section 4. We use 128×128 mesh with trial (2,1) test (2,0). We use Pecklet number $Pe = 1,000,000$ and the wind force $b = 1$. The numerical results are summarized in Figures 4-6.

5. Conclusions

We present a stabilized isogeometric analysis method that exploits the Kronecker product structure of the computational problem. The trial space in our solution

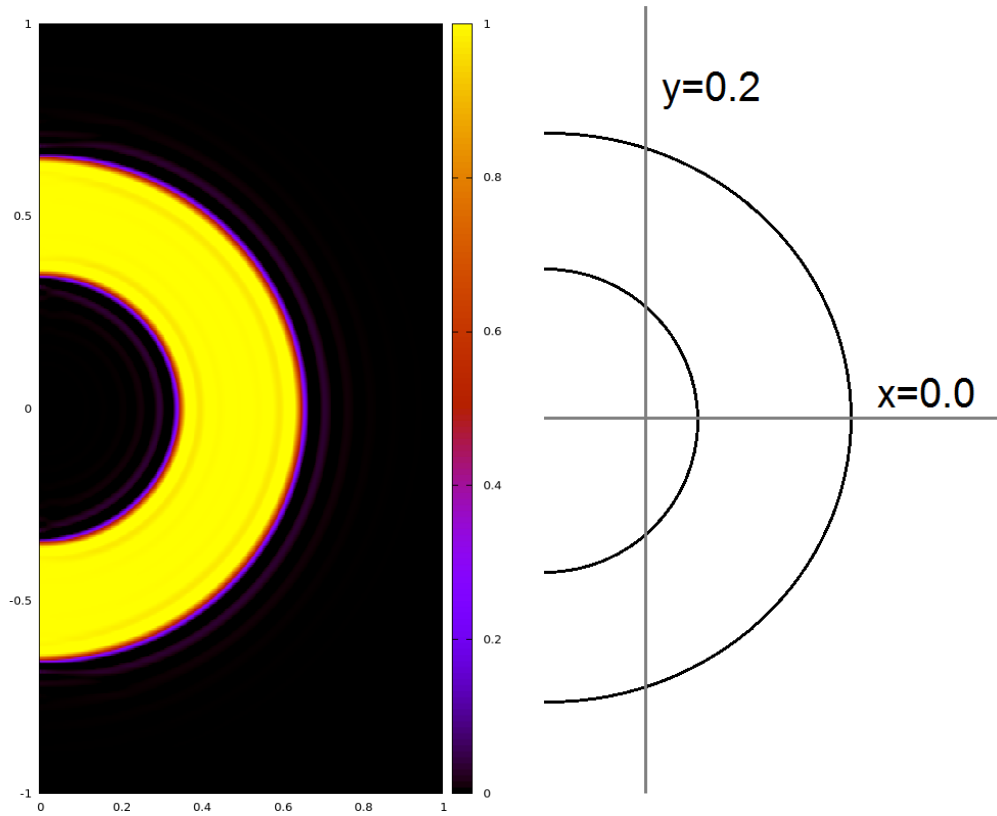


Figure 4: Solution to the circular wind problem on the mesh of 128×128 elements with $\text{trial}(2,1), \text{test}(2,0)$, for Pecklet number $Pe = 1,000,000$, wind force $b = 1$. The locations of cross-sections presented in Figures 5-6.

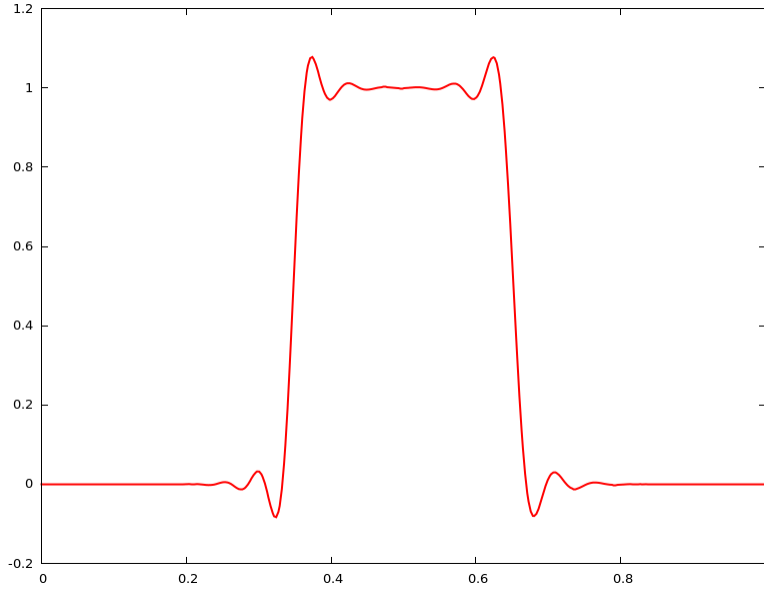


Figure 5: Horizontal cross-section at $x = 0$ through the solution to the circular wind problem on the mesh of 128×128 elements with $\text{trial}(2,1), \text{test}(2,0)$, for Pecklet number $Pe = 1,000,000$, wind force $b = 1$.

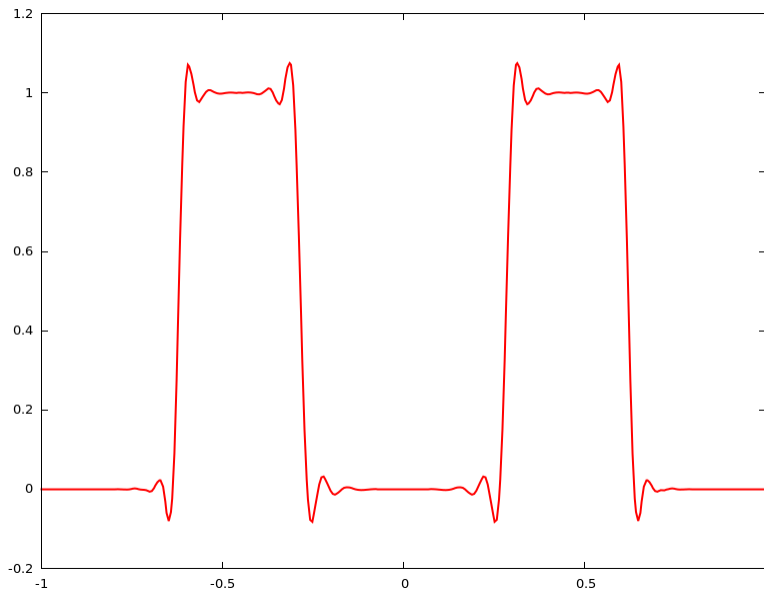


Figure 6: Vertical cross-section at $y = 0.2$ through the solution to the circular wind problem on the mesh of 128×128 elements with $\text{trial}(2,1), \text{test}(2,0)$, for Pecklet number $Pe = 1,000,000$, wind force $b = 1$.

scheme uses maximum continuity B-splines. To accelerate the solution of the algebraic scheme, we introduce preconditioner for the resulting conjugate gradients method which has linear cost. We call our method isogeometric residual minimization (iGRM) with direction splitting preconditioner. We verify the accuracy and efficiency of the solution on four stationary problems, including a problem with an analytical solution, the Eriksson-Johnson problem, and a circular wind problem. In this method, the diffusion and advection coefficient functions can be arbitrary. The problem coefficients do not restrict the efficiency of the solution scheme when they are not Kronecker products. Our future work will extend this method to other problems, such as the Stokes problem [38], and the Maxwell problems [39, 40], the development of the method for time-dependent problems [47], as well as the development of the parallel software dedicated to the simulations of different non-stationary problems with the iGRM method. We will also develop the mathematical foundations on the error analysis, and the convergence of the method.

Acknowledgments

This work is supported by National Science Centre, Poland grant no. 2017/26/M/ST1/00281. This publication was also made possible in part by the CSIRO Professorial Chair in Computational Geoscience at Curtin University and the Deep Earth Imaging Enterprise Future Science Platforms of the Commonwealth Scientific Industrial Research Organisation, CSIRO, of Australia. Additional support was provided by the European Union's Horizon 2020 Research and Innovation Program of the Marie Skłodowska-Curie grant agreement No. 777778, and the Mega-grant of the Russian Federation Government (N 14.Y26.31.0013). Additional, support was provided at Curtin University by The Institute for Geoscience Research (TIGeR) and by the Curtin Institute for Computation. The J. Tinsley Oden Faculty Fellowship Research Program at the Institute for Computational Engineering and Sciences (ICES) of the University of Texas at Austin has partially supported the visits of VMC and MP to ICES.

References

- [1] A. A. Samarskij, E. S. Nikolaev, Numerical Methods for Grid Equations: Volume II Iterative Methods, Birkhuser, Basel, Boston, Berlin (2012)
- [2] A. Quarteroni, R. Sacco, F. Saleri, Numerical Mathematics (Texts in Applied Mathematics) 2nd Edition, Springer, Berlin, Heidelberg, New, York (2006)

- [3] D.W. Peaceman, H.H. Rachford Jr., The numerical solution of parabolic and elliptic differential equations, *Journal of Society of Industrial and Applied Mathematics* 3 (1955) 2841.
- [4] J. Douglas, H. Rachford, On the numerical solution of heat conduction problems in two and three space variables, *Transactions of American Mathematical Society* 82 (1956) 421439.
- [5] E.L. Wachspress, G. Habetler, An alternating-direction-implicit iteration technique, *Journal of Society of Industrial and Applied Mathematics* 8 (1960) 403423.
- [6] G. Birkhoff, R.S. Varga, D. Young, Alternating direction implicit methods, *Advanced Computing* 3 (1962) 189273.
- [7] J. L. Guermond, P. Minev, *A new class of fractional step techniques for the incompressible Navier-Stokes equations using direction splitting*, *Comptes Rendus Mathematique* 348(9-10) (2010) 581585.
- [8] J. L. Guermond, P. Minev, J. Shen, *An overview of projection methods for incompressible flows*, *Computer Methods in Applied Mechanics and Engineering*, 195 (2006) 60116054.
- [9] J. A. Cottrell, T. J. R. Hughes, Y. Bazilevs, *Isogeometric Analysis: Toward Unification of CAD and FEA* John Wiley and Sons, (2009)
- [10] L. Piegl, and W. Tiller, *The NURBS Book (Second Edition)*, Springer-Verlag New York, Inc., (1997).
- [11] L. Dedè, T.J.R. Hughes, S. Lipton, V.M. Calo, *Structural topology optimization with isogeometric analysis in a phase field approach*, USNCTAM2010, 16th US National Congree of Theoretical and Applied Mechanics.
- [12] L. Dedè, M. J. Borden, T.J.R. Hughes, *Isogeometric analysis for topology optimization with a phase field model*, ICES REPORT 11-29, The Institute for Computational Engineering and Sciences, The University of Texas at Austin (2011).
- [13] H. Gómez, V.M. Calo, Y. Bazilevs, T.J.R. Hughes, *Isogeometric analysis of the Cahn-Hilliard phase-field model*, *Computer Methods in Applied Mechanics and Engineering* 197 (2008) 4333–4352.

- [14] H. Gómez, T.J.R. Hughes, X. Nogueira, V.M. Calo, *Isogeometric analysis of the isothermal Navier-Stokes-Korteweg equations*, Computer Methods in Applied Mechanics and Engineering 199 (2010) 1828-1840.
- [15] M.-C. Hsu, I. Akkerman, Y. Bazilevs, *High-performance computing of wind turbine aerodynamics using isogeometric analysis*, Computers and Fluids, 49(1) (2011) 93-100.
- [16] R. Duddu, L. Lavier, T.J.R. Hughes, V.M. Calo, *A finite strain Eulerian formulation for compressible and nearly incompressible hyper-elasticity using high-order NURBS elements*, International Journal of Numerical Methods in Engineering, 89(6) (2012) 762-785.
- [17] K. Chang, T.J.R. Hughes, V.M. Calo, *Isogeometric variational multiscale large-eddy simulation of fully-developed turbulent flow over a wavy wall*, Computers and Fluids, 68 (2012) 94-104.
- [18] S. Hossain, S.F.A. Hossainy, Y. Bazilevs, V.M. Calo, T.J.R. Hughes, *Mathematical modeling of coupled drug and drug-encapsulated nanoparticle transport in patient-specific coronary artery walls*, Computational Mechanics, doi: 10.1007/s00466-011-0633-2, (2011).
- [19] Y. Bazilevs, V.M. Calo, Y. Zhang, T.J.R. Hughes: *Isogeometric fluid-structure interaction analysis with applications to arterial blood flow*, Computational Mechanics 38 (2006).
- [20] Y. Bazilevs, V.M. Calo, J.A. Cottrell, T.J.R. Hughes, A. Reali, G. Scovazzi, *Variational multiscale residual-based turbulence modeling for large eddy simulation of incompressible flows*, Computer Methods in Applied Mechanics and Engineering 197 (2007) 173-201.
- [21] V.M. Calo, N. Brasher, Y. Bazilevs, T.J.R. Hughes, *Multiphysics Model for Blood Flow and Drug Transport with Application to Patient-Specific Coronary Artery Flow*, Computational Mechanics, 43(1) (2008) 161-177.
- [22] L. Gao, V.M. Calo, *Fast Isogeometric Solvers for Explicit Dynamics*, Computer Methods in Applied Mechanics and Engineering, 274 (1) (2014) 19-41.
- [23] L. Gao, V.M. Calo, *Preconditioners based on the alternating-direction-implicit algorithm for the 2D steady-state diffusion equation with orthotropic heterogeneous coefficients*, 273 (1) (2015) 274-295.

- [24] Longfei Gao, Kronecker Products on Preconditioning, PhD. Thesis, King Abdullah University of Science and Technology (2013).
- [25] M. Łoś, M. Woźniak, M. Paszyński, L. Dalcin, V.M. Calo, Dynamics with Matrices Possessing Kronecker Product Structure, *Procedia Computer Science* 51 (2015) 286-295.
- [26] M. Woźniak, M. Łoś, M. Paszyński, L. Dalcin, V. Calo, Parallel fast isogeometric solvers for explicit dynamics, *Computing and Informatics*, 36(2) (2017) 423-448.
- [27] M. Łoś, M. Paszyński, A. Klusek, W. Dzwiniel, Application of fast isogeometric L2 projection solver for tumor growth simulations, *Computer Methods in Applied Mechanics and Engineering*, 316 (2017) 1257-1269.
- [28] M. Łoś, M. Woźniak, M. Paszyński, A. Lenharth, K. Pingali, IGA-ADS : Isogeometric Analysis FEM using ADS solver, *Computer & Physics Communications*, 217 (2017) 99-116.
- [29] G. Gurgul, M. Woźniak, M. Łoś, D. Szeliga, M. Paszyński, Open source JAVA implementation of the parallel multi-thread alternating direction isogeometric L2 projections solver for material science simulations, *Computer Methods in Material Science*, 17 (2017) 1-11.
- [30] P. Bochev, M. Gunzburger, *Least-Squares Finite Element Method*, Springer Applied Mathematical Sciences 166 (2009)
- [31] L. Demkowicz, J. Gopalakrishnan, Recent Developments in Discontinuous Galerkin Finite Element Methods for Partial Differential Equations (eds. X. Feng, O. Karakashian, Y. Xing). In: vol. 157. IMA Volumes in Mathematics and its Applications, (2014). An Overview of the DPG Method, 149180
- [32] A. Cohen, W. Dahmen, G. Welper, *Adaptivity and Variational Stabilization for Convection-Diffusion Equations* *Mathematical Modelling and Numerical Analysis* 46(5) (2012) 1247-1273.
- [33] V. M. Calo, A. Romkes, E. Vålseth, Automatic Variationally Stable Analysis for FE Computations: An Introduction, <https://arxiv.org/abs/1808.01888>
- [34] N. Kopteva, E. O’Riordan, Shishkin meshes in the numerical solution of singularly perturbed differential equations, *International Journal of Numerical Analysis and Modeling*, 7(3) (2010) 393-415.

- [35] J. Chan, J. A. Evans, A minimal-residual finite element method for the convection-diffusion equations, ICES-REPORT 13-12 (2013)
- [36] V. M. Calo, Residual-based multiscale turbulence modeling: Finite volume simulations of bypass transition, Stanford University, Ph.D. Thesis (2005)
- [37] T.J.R. Hughes, L.P. Franca, M. Mallet, A new finite element formulation for fluid dynamics: VI. Convergence analysis of the generalized SUPG formulation for linear time dependent multidimensional advectivediffusive systems, Computer Methods in Applied Mechanics and Engineering, 6 (1987) 97112.
- [38] J. Evans, T. J. R. Hughes, Isogeometric divergence-conforming B-splines for the Darcy–Stokes–Brinkman equations, Mathematical Models and Methods in Applied Sciences, 23(4) (2013) 671-741.
- [39] M. Hochbruck, T. Jahnke, R. Schnaubelt, Convergence of an ADI splitting for Maxwell’s equations, Numerische Mathematik, 129 (2015) 535-561.
- [40] G. Liping, Stability and Super Convergence Analysis of ADI-FDTD for the 2D Maxwell Equations in a Lossy Medium, Acta Mathematica Scientia, 32(6) (2012) 2341-2368.
- [41] J. Nocedal, S. J. Wright, Conjugate gradient methods, Numerical optimization (2006) 101-134.
- [42] Horn, R. A., Horn, R. A., Johnson, C. R., Matrix analysis. Cambridge university press. (1990)
- [43] P. R. Amestoy , I. S. Duff, *Multifrontal parallel distributed symmetric and unsymmetric solvers*, Computer Methods in Applied Mechanics and Engineering, 184 (2000) 501-520.
- [44] P. R. Amestoy, I. S. Duff, J. Koster, J.Y. L’Excellent, *A fully asynchronous multifrontal solver using distributed dynamic scheduling*, SIAM Journal of Matrix Analysis and Applications, 1(23) (2001) 15-41.
- [45] P. R. Amestoy, A. Guermouche, J.-Y. L’Excellent, S. Pralet, *Hybrid scheduling for the parallel solution of linear systems*, Computer Methods in Applied Mechanics and Engineering, 2(32) (2001) 136-156.

- [46] Y. Bazilevs, C. Michler, V. M. Calo, T.J.R. Hughes, Isogeometric variational multiscale modeling of wall-bounded turbulent flows with weakly enforced boundary conditions on unstretched meshes, *Computer Methods in Applied Mechanics and Engineering* 199(13-16) (2008) 780-790.
- [47] M. Łoś, , J. Muñoz-Matute, I. Muga, M. Paszyński, Isogeometric Residual Minimization Method (iGRM) with Direction Splitting for Non-Stationary Advection-Diffion Problems, submitted to *Computers and Mathematics with Applications* (2019).
- [48] T.J.R. Hughes, J.A. Cottrell, Y. Bazilevs. Isogeometric analysis: CAD, finite elements, NURBS, exact geometry and mesh refinement, *Computer Methods in Applied Mechanics and Engineering*, (39-41) 4135-4195 (2005)